Colorimetric Immunological Paper-based Assay for Exosome Detection

Surasak Kasetsirikul
Griffith University https://orcid.org/0000-0001-9767-1254
Muhammad J.A. Shiddiky (m.shiddiky@griffith.edu.au)
Griffith University https://orcid.org/0000-0002-9461-9888
Nam-Trung Nguyen (nam-trung.nguyen@griffith.edu.au)
Griffith University https://orcid.org/0000-0003-3626-5361

Research Article

Keywords: Exosome detection, Paper-based diagnostic device, Colorimetric assay

Posted Date: October 6th, 2021

DOI: https://doi.org/10.21203/rs.3.rs-956090/v1

Abstract

This paper reports the development of colorimetric immunological paper-based assay for exosome detection. The paper-based device was fabricated with lamination technique for easy handling and create hydrophilic/hydrophobic region for analytical paper-based devices. Exosome-specific antibody was coated onto the paper-based devices as a biosensing platform to detect exosome sample from the cell culture media. This assay employed a colorimetric reaction which is followed by reaction between horseradish peroxidase (HRP) and 3,3',5,5'-tetramethylbenzidine substrate (TMB). The colorimetric readout was qualitatively evaluated by naked eyes and was quantitatively assessed by image processing software. The result indicated that this assay faces many challenges. First, the exosome concentration may be inadequate to reach detectable range. Second, high background signal due to non-specific binding on the platform results in lack of sensitivity for exosome detection. Therefore, modification on the paper should promote protein binding for specific target and prevent non-specific binding to reduce the high background signal.

1. Introduction

Exosomes secreted as extracellular vesicles from most cell types which are 30 – 150 nm in diameter.[1–4] Exosomes contain many biomolecules such as proteins, lipids and various types of nucleic acids playing a role in cell-cell interaction. Generally, exosomes are released by most cell types and circulated in biological fluids such as saliva, blood, and urine. Recent studies suggested that these exosomes play a significant role in many pathological processes such as cancers [5], pregnancy complications [6, 7] and neurodegenerative diseases [8]. Recently, exosomal proteins have served as diagnostic cancer biomarkers. [9–12] Some cancer-derived exosome can be detection due to specific antibody proteins on exosomal membrane such as CA-125, EpCAM for ovarian cancer [13], or CD24, EDIL3, fibronectin for breast cancer [10]. Additionally, the number of exosomes in unhealthy samples is significantly higher than healthy one [7].

Therefore, isolation, purification and analysis of disease-specific exosomes have been attracted a great deal of attentions from many research groups in recent years [14]. Due to the physical and biochemical properties of exosomes, the effective isolation of exosomes from bodily fluids is still challenging [15]. Conventional methods such as gradient density centrifugation, ultrafiltration or immunological separation have been performed [16, 17]. However, these centrifugal isolations require a few hours and expensive equipment which may be unavailable in low-resource settings. In addition to centrifugal method, commercial isolation kits are also available. These kits avoid time-consuming procedure and using expensive facilities by precipitating exosome with polyethylene glycol or related chemicals [18]. Nonetheless, the final product may be contaminated with chemicals from the kits which may influence the downstream analysis. Alternatively, nanoparticle tracking analysis (NTA) [19, 20], flow cytometry [21, 22], electrochemical-based approaches [23, 24], Enzyme-linked immunosorbent assay (ELISA) [25, 26] and are successfully demonstrated to quantify and detect exosome. ELISA is known as a conventional method to detect and analyse various biomolecules, based on immunological assay between antibodies

and protein on exosome membranes. However, the standard protocol is time consuming with laborious sample loading, washing, and incubation step.

Paper-based platform enables a number of microfluidic sample preparation tasks such as preconcentration and heating [27, 28]. Recently, paper-based ELISA is promising for diagnostic application due to low cost, friendly use and small sample need was successfully demonstrated for detecting antibodies and exosomes application [29–32]. In limited-resource environments, colorimetric assay is useful and easily observed by naked eyes. One of commonly used colorimetric reactions is 3,3’,5,5’-tetramethylbenzidine substrate and horseradish peroxidase (TMB/HRP). TMB/HRP reaction produces a colour product in the presence of target biomolecules conjugated with HRP [33]. Therefore, this study developed paper-based ELISA assay for exosome detection. The target was captured with exosome-specific antibody and formed immunological complex on the paper. The colorimetric readout relies on TMB/HRP reaction resulting from HRP-conjugated antibody.

2. Materials And Methods

2.1 Materials and chemicals

Paper materials used as a platform device in this study were chromatography filter paper (CHR, Whatman, UK), and nitrocellulose membrane with laminated backing support (NC, FF180HP, Merck, USA). Gloss laminate pouch with 80-µm thickness (GBC, Australia) were used to make paper hydrophobic. For immunological assay, Rabbit monoclonal anti-human CD9 (Rabbit Anti-CD9, ab92726, Abcam, UK), Goat anti-rabbit IgG (Anti-rabbit IgG, ab6721, Abcam, UK), Mouse monoclonal Anti-human CD63 conjugated with horseradish peroxidase (Anti-CD63-HRP, NBP2-42225H, Novus, USA) were used for coating and detecting antibody. HRP-conjugation kit (ab102890, Abcam, UK) was used to conjugate HRP onto an antibody. For blocking paper-based assay, Bovine Serum Albumin (BSA, A1595, Sigma Aldrich, USA) was used to block the assay to minimize background signal due to non-specific binding. 3,3’,5,5’-tetramethylbenzidine substrate solution (TMB, 002023, Thermo Fisher Scientific, Germany) was used to employ colorimetric immunological assay, employed by HRP/TMB reaction. For general chemical usage, phosphate buffer saline solution (PBS) was prepared by dissolving phosphate buffer saline tablet (10388739, Fisher Scientific, USA) in deionized water (DI water, Milli-Q, Merck, USA). Tween-20 (655205, Merck, USA) as a surfactant was mixed into PBS for preparing PBST (0.05% Tween-20 in PBS).

For exosome preparation, SKOV3 (ovarian cancer cells, ATCC, USA), OVCAR3 (ovarian cancer cells, ATCC, USA), HEK293 (epithelial human cells, ATCC, USA) and Met5a (epithelial human cells, ATCC, USA) were used as a cell line to produce exosome. RPMI-1640 media (11875-093, Gibco, Thermo Fisher Scientific, Germany) served as the base medium. Foetal Bovine Serum (FBS, A3160901, Gibco, Thermo Fisher Scientific, Germany) and Exosome-depleted Foetal Bovine Serum (Exosome-free FBS, A25904DG, Gibco, Thermo Fisher Scientific, Germany) were used as a main composition for cell culture medium. To prevent bacterial and fungal contamination, 1% Penicillin and Streptomycin (PenStrep, 15140-122, Gibco, Thermo Fisher Scientific, Germany) was mixed into the cell culture medium. TrypLE (12604-021, Gibco, Thermo

Fisher Scientific, Germany) was used for trypsinization process for subculturing. General buffer for washing cells was sterile HBSS (14175-095, Gibco, Thermo Fisher Scientific, Germany). After exosome isolation, exosome sample was purified by using Total Exosome Isolation Kits (4478359, Invitrogen, Thermo Fisher Scientific, Germany). MCF7 standard exosome (MCF7, ab239691, Abcam, UK) was used to validate the exosome detection assay.

2.2 Paper-based device fabrication

The designed pattern on paper was drawn by CorelDRAW software (CorelDRAW2019, Corel Corporation Inc, Canada), and then the paper was cut with laser cutting machine (Rayjet 50 Laser Engraver, Rayjet, Australia). In this study, we fabricated three types of paper devices for different experiments. First, NC without lamination, a paper platform which is NC only was directly cut by laser cutting machine. Second, with lamination device (Figure 1), CHR paper were cut with 5-mm diameter piece. A laminated film was cut with the hole of 4-mm diameter. After the paper was aligned into the centre of laminated film hole, the aligned component was fed into a laminator (JL330T, PFEC, Australia) at 130^{o}C and at a speed of 10 mm/s. Finally, the paper device was cut into individual device.

2.3 Exosome sample preparation

SKOV3, OVCAR3, HEK293 and Met5a were cultured with RPMI-1640 containing 10% FBS and 1% PenStrep. After reaching 80% confluence, the media was changed to exosome-free media which is RPMI-1640 consisting of 10% exosome-depleted FBS. After cells were incubated with exosome-free media for 60 hours, the media was collected and centrifuged at 2,000 g for 30 min to remove dead cells and other debris. The exosome isolation kit was used to precipitate the exosome to increase the exosome concentration from the collected media. Before obtaining exosome pellet by centrifugation at 10,000 g for 1 hour, the mixture was incubated overnight. After the centrifugation process, the exosome pellet was acquired by discarding the supernatant, resuspended with PBS and kept in -80^{o}C for long-term storage.

2.4 Colorimetric assay for exosome detection

In this study, we employed sandwich ELISA assay on a paper-based platform using TMB/HRP colorimetric reactions. Briefly, the primary antibody specific to tetraspanin family on exosome membrane e.g. CD9 or CD63 was firstly immobilized onto the paper. Then, the paper was blocked by BSA or NFM to minimize non-specific binding. Subsequently, exosome sample was loaded and incubated onto the paper to allow to be captured by primary antibody using affinity between primary antibody and specific protein on exosome membrane. Subsequently, the secondary antibody which is tagged with HRP was loaded to attach onto exosome membrane. Next, TMB substrate will be added onto the paper to employ TMB/HRP reaction. In the presence of HRP, TMB was oxidized by the HRP and generated blue colour from colourless solution. On the other hand, in the absence of HRP, TMB was inert and left solution to be colourless.

2.5 Equipment setup and data acquisition

As the experimental results are evaluated based on colour change from TMB/HRP reaction, the paper device was observed under 1.3 megapixels TOUPCAM camera (UCMOS01300KPA, Touptek, China) with

1/3” Aptina CMOS sensor attached with 6.2 mm focal lens (58428, Edmund Optics Inc, USA) for image acquisition (Figure 2) under LED strip box made from PMMA for light control. Camera setup was connected via USB and controlled by Toupview software (Version 4.8, Touptek, China). Image processing was quantified with programming code in computing software (MATLAB R2018b, The MatkWorks Inc, USA)

2.6 Experimental design and assay optimization

2.6.1 Blocking efficiency test

Most colorimetric assays involve with enzyme incubation, so blocking and washing are important steps to prevent non-specific binding. We evaluated the blocking capability by coating different BSA concentrations. A volume of 5 µL of blocking solution was added to incubate for 10 min and subsequently dry for 10 min. Next, we dropped Anti-CD63-HRP for 3 minutes onto the paper and washed it subsequently. Finally, we incubated TMB substrate and observed colour change over time. It is anticipated that the best condition for blocking could result in the lowest intensity of blue colour change. The first configuration is to incubate NC paper without lamination into different BSA concentrations from 1–10% for 30 min in dipping configuration. In this case, we used only NC paper because we take advantage of high protein binding of NC materials. Moreover, we also evaluated the blocking capability by dropping and incubating BSA onto laminated CHR paper with wash-through configuration.

After getting optimal blocking condition, we investigated antibody binding capability. We dropped 5 µL of 0.1 mg/mL rabbit anti-human CD9 on a laminated paper and incubate for 10 minutes, then dry at 37^{o}C for 10 minutes. Next, coated antibody laminated paper was blocked with BSA. In the presence of rabbit anti-human CD9, we expected that after loading goat anti-rabbit IgG conjugated with HRP, TMB could change from colourless to blue colour due to in the presence of rabbit anti-human CD9 on paper. However, In the absence of rabbit anti-human CD9, TMB could remain colourless as there is no binding of goat anti-rabbit IgG conjugated with HRP.

2.6.2 Analytical performance assay

After obtaining optimal condition for blocking and paper type for the paper-based device, we carried out the analytical performance assay. Assay preparation including antibody concentration and operation procedure were adapted from the previous study (Figure 3a). [31] We dropped 5 µL of 0.1 mg/mL rabbit anti-human CD9 on a laminated paper and incubate for 10 min, then drird at 37^{o}C for 10 minutes. Next, we dropped 5 µL of 2% BSA on the laminated paper. Subsequently, we incubated exosome sample on the paper for 10 minutes. In the absence of exosomes in the sample, PBS was used as control. Subsequently, we loaded 3 µL of 1 µg/mL Anti-CD63-HRP for 3 min. Finally, we added TMB substrate and placed under the camera and captured photos at 1st, 3rd, 5th, 10th, 15th, and 20th minute.

2.7 Data processing and quantification

After adding TMB onto the paper device, the assay was placed under the camera. Qualitative data were observed as the change in colour due to the TMB/HRP reaction. For quantitative data, all images were quantified and processed with MATLAB. Briefly, the individual image was imported by MATLAB. The area of interest was defined by cropping the image. The original RGB colour image was split into R, G and B channels as grayscale images.

Next, the mean grey value ΔRGB was estimated for each channel as:

$$\Delta RGB = \sqrt{(R - R_0)^2 + (G - G_0)^2 + (B - B_0)^2}$$

1

,

where R, G and B are the mean grey value from arbitrary images of red, green, blue channel respectively. The mean grey values R_0, G_0 and B_0 are of the red, green, blue channels of the control sample, respectively. To make sure that the colour change only results from the assay, the RGB value reported in this study was subtracted by background signal from negative samples as:

$$RGBvalue = \Delta RGB - \Delta RGB_{neg}$$

2

where ΔRGB is the mean grey value of the sample and ΔRGB_{neg} is the mean grey value of the negative sample, calculated from Eq. (1). All experiments were performed with at least a sample number of n = 3. The error bars were determined by the standard deviation.

3. Result And Discussion

3.1 Consistency of image quality observed by the system

As photo quality and image acquisition method are important for colorimetric assay, we also investigated the quality of the image according to our experiment setup. We evaluated the mean grey value of all green, red, blue channels from 14 different CHR paper samples (Figure 4) as well as the system was switch on and off for taking every photo. This system showed that the average value of mean grey values of 14 samples with small standard deviation (less than 1% of the average value). small variation from quantitative data. Therefore, this equipment setup for image acquisition is consistent to get the same image quality by having small variation of mean grey value.

3.2 Evaluation of blocking capability

Blocking is an important step to prevent non-specific absorption. Blue colour development results from the reaction between TMB and sequential antibody conjugated with HRP. For dipping configuration of NC

paper, the blue colour was developed overtime for 1 - 10% BSA concentrations. However, the quantitative data quantified by MATLAB showed that 2% BSA provided the lowest ΔRGB which corresponds to the lowest amount of Anti-human CD63-HRP left on the paper (Figure 5). Nevertheless, the background signal was still high because NC has high protein binding capacity. [34–36] Moreover, washing method for dipping configuration could be another factor that sequential antibody was still on the paper. Dipping a paper device into PBS in 96-well plate may just only diluted the antibody on the paper or surface tension acting between NC surface and PBS in the 96-well plate may not enough to remove non-binding antibody and may still be on the paper. For these reasons, NC paper may not be appropriate for colorimetric immunological paper-based assay because sequential antibody was able to absorb non-specifically and difficult to be removed from the paper. Thus, we redesigned the paper platform by making wash-through configuration so that non-adherent molecules could be wash out. Unfavourably, NC paper in this study was back-laminated, so NC cannot make wash-through configuration. Nonetheless, 2% BSA was selected to be used for further studies because it provided the smallest background signal generated from non-specific binding.

3.3 Evaluation of antibody binding efficiency

Even though NC paper acquires high protein binding capacity, it produced high background signal due to non-specific binding. Thus, we also reevaluated antibody binding capacity and blocking performance for CHR paper. In the presence of rabbit anti-human CD9, goat anti-rabbit IgG-HRP was captured by primary antibody and reacted with TMB solution to generate blue colour from colourless. In the absence of goat rabbit anti-human CD9, anti-rabbit IgG-HRP was washed away as there is no specific binding between primary and secondary antibodies. Laminated CHR paper (L-CHR) in the absence of rabbit anti-human CD9 had lighter blue colour than L-CHR in the presence of rabbit anti-human CD9. It represented that blocking with 2% BSA on L-CHR could prevent non-specific binding. Additionally, 0.1 mg/mL rabbit anti-human CD9 was well immobilised on the paper resulting in blue colour generation from reaction between Anti-rabbit IgG-HRP and TMB.

3.4 Analytical performance of the assay

Colorimetric immunological assay for exosome detection by employed TMB/HRP reaction. The presence of detecting antibody conjugated with HRP in the assay enables the oxidation of TMB and generates blue-colour complex. To validate exosome colorimetric immunological detection assay, we performed the assay with a sample containing exosomes harvested from cell culture media (positive control), while a negative control sample without exosomes was PBS only (see Figure 7). However, there is no significant difference between positive and negative control for MCF standard exosome, OVCAR3, SKOV3, Met5a and HEK293 exosome samples in unmodified L-CHR. This result could originate from several issues. First, the concentration of exosome sample may be inadequate to reach detectable range. The exosome samples collected from cell culture media were quantified using NanoSight NS300 (NanoSight Ltd., Amesbury, UK) to determine the concentration in the range 10^8-10^9 exosome/mL. (See in supplementary information section S.1) Nevertheless, limit of detection for exosome detection with colorimetric assay

referring to previous studies was in the range of 10^8 exosome/mL [32]. Second, high background signal was also found in paper-based ELISA assay [30–32]. As a result, the blue-colour generation from negative control coming from non-specific binding is similar or higher than positive control. Protein binding enhancement to provide more specific detection and prevent non-specific binding could be one of possible ways to strengthen protein affinity between paper-based matrix and antibodies. Thus, we proposed physical and chemical modification on paper to validate the colorimetric exosome detection assay.

4. Conclusion

We have developed and studied an inexpensive colorimetric paper-based assay for exosome detection. Colorimetric readout facilitates naked-eye observation and can be quantified by image processing. With the proof-of-concept, we encountered various challenges in assay optimization and development to detect exosomes. First, exosome concentration from cell culture may be inadequate for colorimetric paper-based assay. Due to recent study by Lee et al (2020), the limit of detection was also in the similar range to the concentration collected from the cell culture media [32]. Second, the background signal from non-specific binding was high, as the paper is a three-dimensional structure that possibly promote HRP-conjugated antibody left over in the matrix after washing. Therefore, we may need to engineer the paper physically or chemically to both strengthen detecting antibody binding on paper matrix and prevent non-specific binding to reduce background signal. Physical modification such as casting nanomaterials may promote the strength of detecting antibody to be bound on the paper platform to allow the assay to be more specific to the samples [37, 38]. On the other hand, chemical modification may add more functional group to promote protein binding such as EDC/NHS or APTES treatment [39–41]. However, antibody and protein conjugation to nanomaterials as well as applicability to detect low concentration of exosomes require a huge batch of optimization work.

Declarations

5. Acknowledgement

The authors acknowledge the support of the Australian Research Council (DP180100055) and higher degree research scholarships GUIPRS and GUPRS Scholarships to S.K. from the Griffith University.

Competing Interests: The authors declare no competing interests.

References

1. Anand, P.K., *Exosomal membrane molecules are potent immune response modulators*. Communicative & integrative biology, 2010. **3**(5): p. 405–408.
2. Sokolova, V., et al., *Characterisation of exosomes derived from human cells by nanoparticle tracking analysis and scanning electron microscopy*. Colloids and Surfaces B: Biointerfaces, 2011. **87**(1):

p. 146–150.

3. Valadi, H., et al., *Exosome-mediated transfer of mRNAs and microRNAs is a novel mechanism of genetic exchange between cells*. Nature Cell Biology, 2007. **9**(6): p. 654–659.
4. Soda, N., et al., *Advanced liquid biopsy technologies for circulating biomarker detection*. Journal of Materials Chemistry B, 2019. **7**(43): p. 6670–6704.
5. Skog, J., et al., *Glioblastoma microvesicles transport RNA and proteins that promote tumour growth and provide diagnostic biomarkers*. Nature cell biology, 2008. **10**(12): p. 1470–1476.
6. Salomon, C., et al., *Placental Exosomes as Early Biomarker of Preeclampsia: Potential Role of Exosomal MicroRNAs Across Gestation*. The Journal of Clinical Endocrinology & Metabolism, 2017. **102**(9): p. 3182–3194.
7. Salomon, C., et al., *Gestational Diabetes Mellitus Is Associated With Changes in the Concentration and Bioactivity of Placenta-Derived Exosomes in Maternal Circulation Across Gestation*. Diabetes, 2016. **65**(3): p. 598.
8. *Alzheimer's disease β-amyloid peptides are released in association with exosomes.* Proceedings of the National Academy of Sciences, 2006. **103**(30): p. 11172.
9. Rice, G.E., et al., *The Effect of Glucose on the Release and Bioactivity of Exosomes From First Trimester Trophoblast Cells*. The Journal of Clinical Endocrinology & Metabolism, 2015. **100**(10): p. E1280-E1288.
10. Rupp, A.-K., et al., *Loss of EpCAM expression in breast cancer derived serum exosomes: Role of proteolytic cleavage*. Gynecologic Oncology, 2011. **122**(2): p. 437–446.
11. Soung, Y.H., et al., *Exosomes in Cancer Diagnostics.* Cancers, 2017. **9**(1).
12. Truong, G., et al., *Oxygen tension regulates the miRNA profile and bioactivity of exosomes released from extravillous trophoblast cells – Liquid biopsies for monitoring complications of pregnancy*. PLOS ONE, 2017. **12**(3): p. e0174514.
13. Cheruvanky, A., et al., *Rapid isolation of urinary exosomal biomarkers using a nanomembrane ultrafiltration concentrator*. American journal of physiology. Renal physiology, 2007. **292**(5): p. F1657-F1661.
14. Boriachek, K., et al., *An amplification-free electrochemical detection of exosomal miRNA-21 in serum samples*. Analyst, 2018. **143**(7): p. 1662–1669.
15. Lötvall, J., et al., *Minimal experimental requirements for definition of extracellular vesicles and their functions: a position statement from the International Society for Extracellular Vesicles*. Journal of Extracellular Vesicles, 2014. **3**(1): p. 26913.
16. Clayton, A., et al., *Analysis of antigen presenting cell derived exosomes, based on immuno-magnetic isolation and flow cytometry*. Journal of Immunological Methods, 2001. **247**(1): p. 163–174.
17. Merchant, M.L., et al., *Microfiltration isolation of human urinary exosomes for characterization by MS*. PROTEOMICS – Clinical Applications, 2010. **4**(1): p. 84–96.

18. van der Pol, E., et al., *Recent developments in the nomenclature, presence, isolation, detection and clinical impact of extracellular vesicles*. Journal of Thrombosis and Haemostasis, 2016. **14**(1): p. 48–56.
19. Dragovic, R.A., et al., *Sizing and phenotyping of cellular vesicles using Nanoparticle Tracking Analysis.* Nanomedicine: nanotechnology, biology, and medicine, 2011. **7**(6): p. 780-788.
20. Soo, C.Y., et al., *Nanoparticle tracking analysis monitors microvesicle and exosome secretion from immune cells*. Immunology, 2012. **136**(2): p. 192–197.
21. Erdbrügger, U. and J. Lannigan, *Analytical challenges of extracellular vesicle detection: A comparison of different techniques*. Cytometry Part A, 2016. **89**(2): p. 123–134.
22. Lacroix, R., et al., *Overcoming Limitations of Microparticle Measurement by Flow Cytometry*. Seminars in Thrombosis and Hemostasis, 2010. **36**(8): p. 807–818.
23. Boriachek, K., et al., *Avoiding Pre-Isolation Step in Exosome Analysis: Direct Isolation and Sensitive Detection of Exosomes Using Gold-Loaded Nanoporous Ferric Oxide Nanozymes*. Analytical Chemistry, 2019. **91**(6): p. 3827–3834.
24. Yadav, S., et al., *An Electrochemical Method for the Detection of Disease-Specific Exosomes*. ChemElectroChem, 2017. **4**(4): p. 967–971.
25. Khan, S., et al., *Early diagnostic value of survivin and its alternative splice variants in breast cancer*. BMC Cancer, 2014. **14**(1): p. 176.
26. Logozzi, M., et al., *High Levels of Exosomes Expressing CD63 and Caveolin-1 in Plasma of Melanoma Patients*. PLOS ONE, 2009. **4**(4): p. e5219.
27. Dinh, T., et al., *Graphite on paper as material for sensitive thermoresistive sensors*. Journal of Materials Chemistry C, 2015. **3**(34): p. 8776–8779.
28. Phan, D.-T., et al., *Sample concentration in a microfluidic paper-based analytical device using ion concentration polarization*. Sensors and Actuators B: Chemical, 2016. **222**: p. 735–740.
29. Chen, C., et al., *Paper-based devices for isolation and characterization of extracellular vesicles*. Journal of visualized experiments: JoVE, 2015(98): p. e52722-e52722.
30. Cheng, C.-M., et al., *Paper-Based ELISA*. Angewandte Chemie International Edition, 2010. **49**(28): p. 4771–4774.
31. Kasetsirikul, S., et al., *Detection of the SARS-CoV-2 humanized antibody with paper-based ELISA*. Analyst, 2020. **145**(23): p. 7680–7686.
32. Lee, J., et al., *Enhanced paper-based ELISA for simultaneous EVs/exosome isolation and detection using streptavidin agarose-based immobilization*. Analyst, 2020. **145**(1): p. 157–164.
33. Koo, K.M., E.J.H. Wee, and M. Trau, *Colorimetric TMPRSS2-ERG Gene Fusion Detection in Prostate Cancer Urinary Samples via Recombinase Polymerase Amplification*. Theranostics, 2016. **6**(9): p. 1415–1424.
34. Nakamura, K., T. Tanaka, and K. Takeo, *Characterization of protein binding to a nitrocellulose membrane*. Seibutsu Butsuri Kagaku, 1989. **33**: p. 293–303.

35. Tonkinson, J. and B.A. Stillman, *Nitrocellulose: a tried and true polymer finds utility as a post-genomic substrate*. Frontiers in bioscience: a journal and virtual library, 2002. **7**: p. c1-12.
36. Tovey, E.R. and B.A. Baldo, *Protein binding to nitrocellulose, nylon and PVDF membranes in immunoassays and electroblotting*. Journal of Biochemical and Biophysical Methods, 1989. **19**(2): p. 169–183.
37. Bulbul, G., H. Eskandarloo, and A. Abbaspourrad, *A novel paper based colorimetric assay for the detection of TiO2 nanoparticles*. Analytical Methods, 2018. **10**(3): p. 275–280.
38. Nguyen, Q.H. and M.I. Kim, *Nanomaterial-mediated paper-based biosensors for colorimetric pathogen detection*. TrAC Trends in Analytical Chemistry, 2020. **132**: p. 116038.
39. Butwong, N., et al., *Silver-doped CdS quantum dots incorporated into chitosan-coated cellulose as a colorimetric paper test stripe for mercury*. Microchimica Acta, 2018. **185**(2): p. 126.
40. Gomes, H.I.A.S. and M.G.F. Sales, *Development of paper-based color test-strip for drug detection in aquatic environment: Application to oxytetracycline*. Biosensors and Bioelectronics, 2015. **65**: p. 54–61.
41. Piovesan, C., et al., *Paper strengthening by polyaminoalkylalkoxysilane copolymer networks applied by spray or immersion: a model study*. Cellulose, 2014. **21**(1): p. 705–715.

Figures

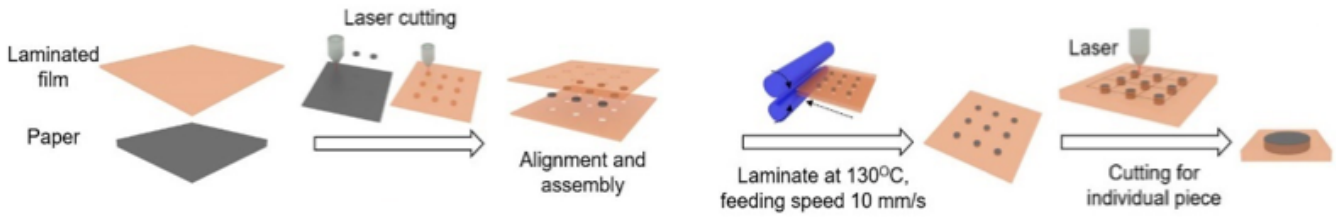

Figure 1

Schematic diagram of paper fabrication with lamination for colorimetric immunological paper-based assay.

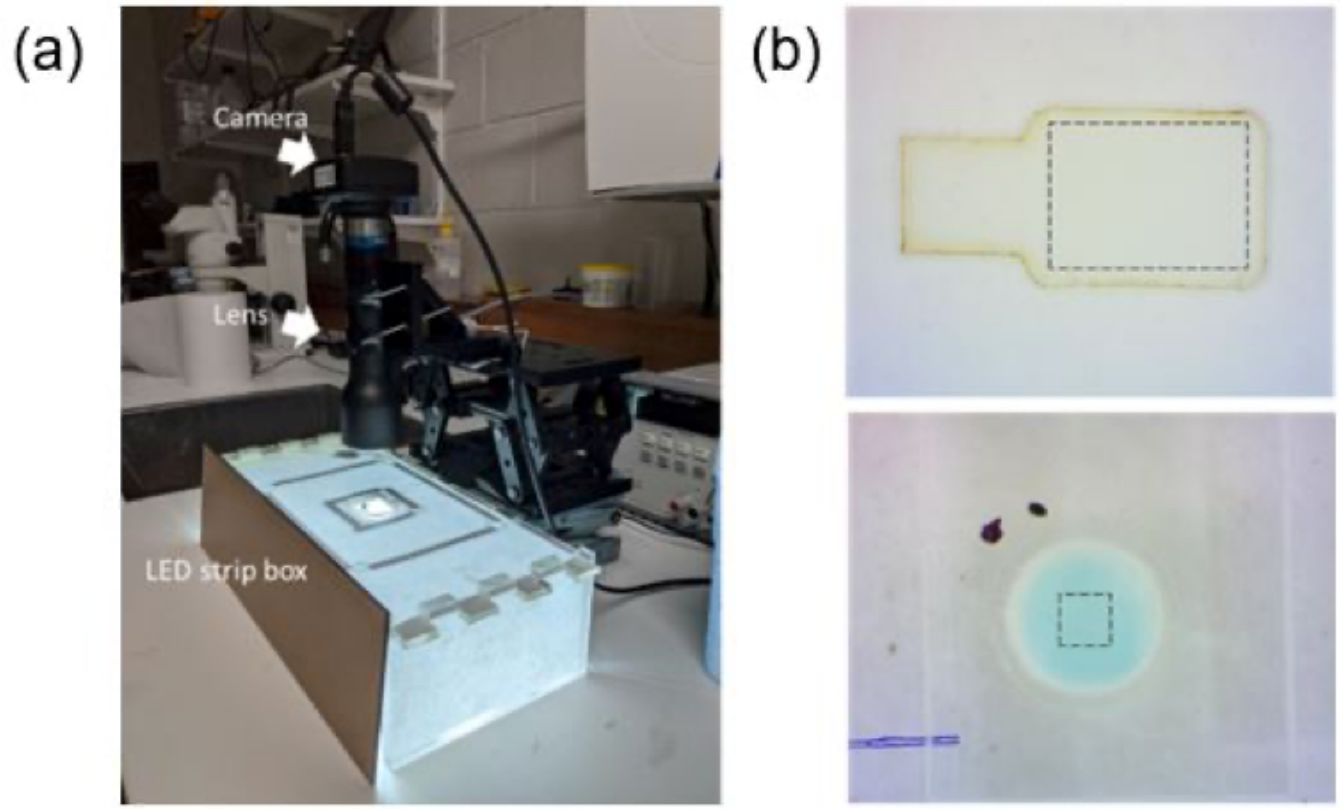

Figure 2

(a) Experimental setup and data acquisition system containing LED Strip box and camera to observe colour change on colorimetric immunological paper-based device (b) Images obtained from the camera were imported into MATLAB and processed before quantification inside dash box lines which were an area of interest.

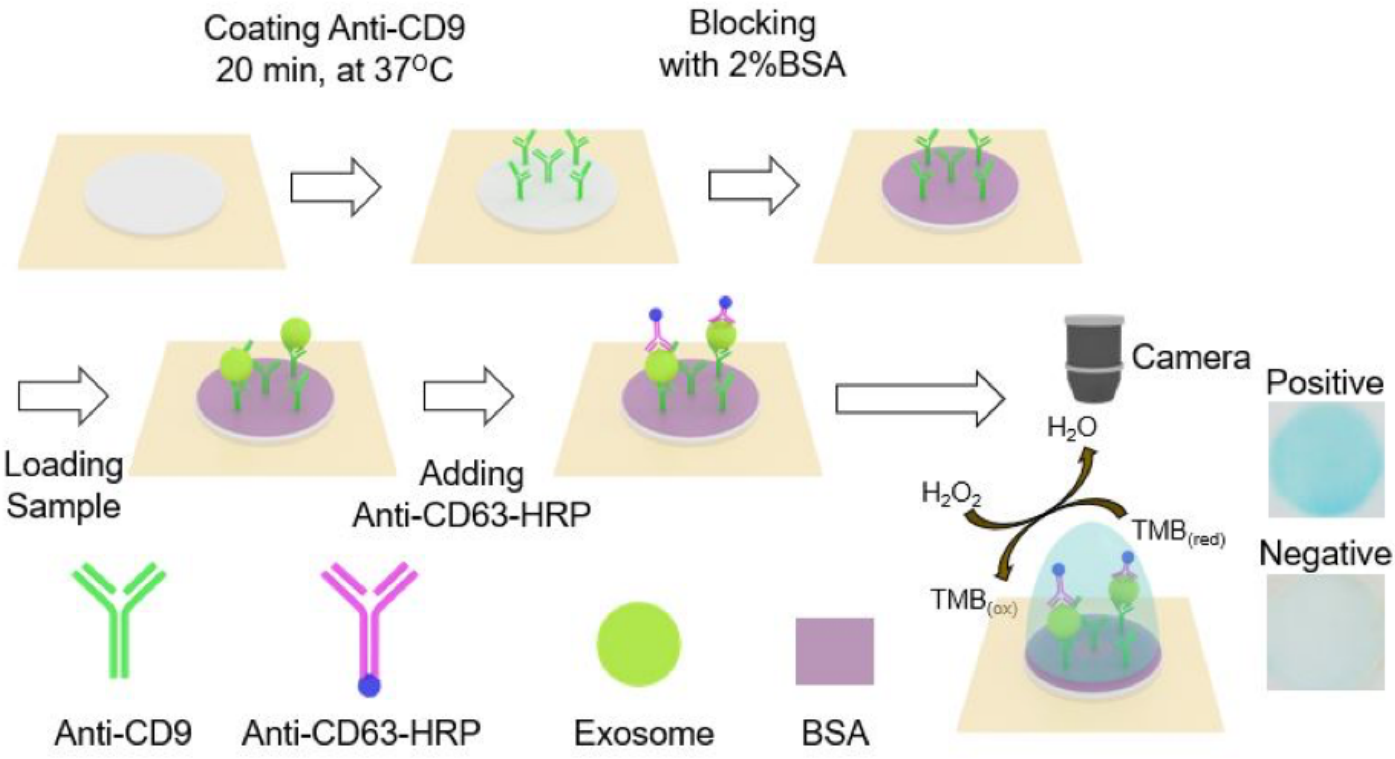

Figure 3

Schematic Diagram of preparation process of paper-based device for exosome detection. The paper was coated with anti-human CD9 to capture exosomes. HRP/TMB reaction was employed to validate colorimetric assay.

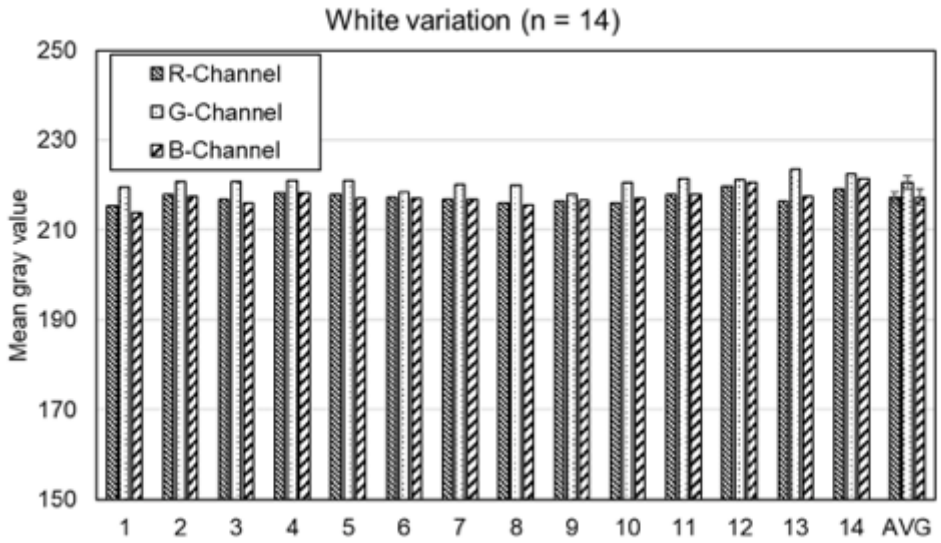

Figure 4

The consistency of image quality taken by the experimental setup was reported by mean grey value from 14 different CHR samples.

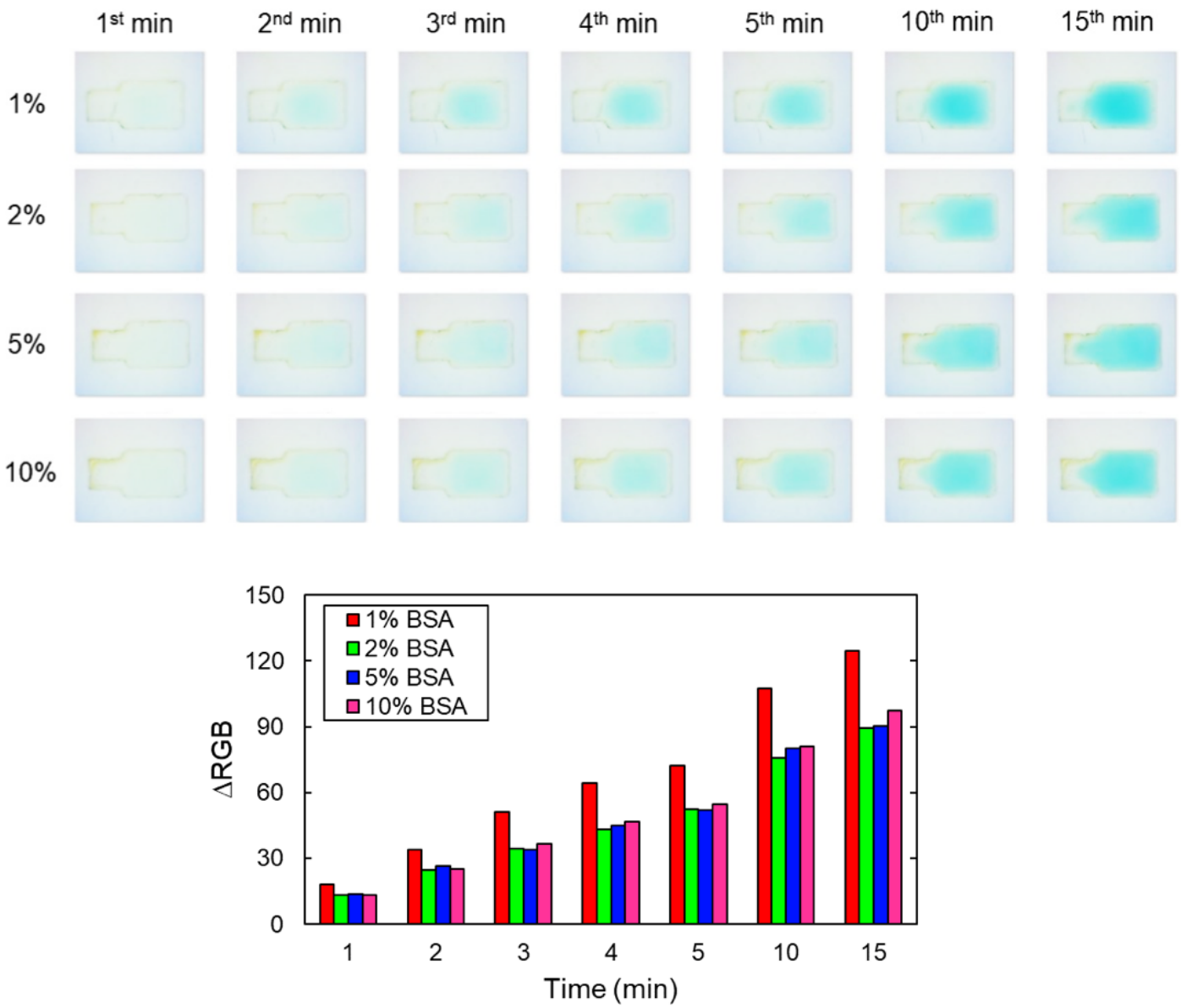

Figure 5

The sequential images of 1% to 10% BSA blocking on NC paper over time. The bar diagram for ΔRGB observed in 1st, 2nd, 3rd, 4th, 5th, 10th, and 15th min from various blocking BSA concentration.

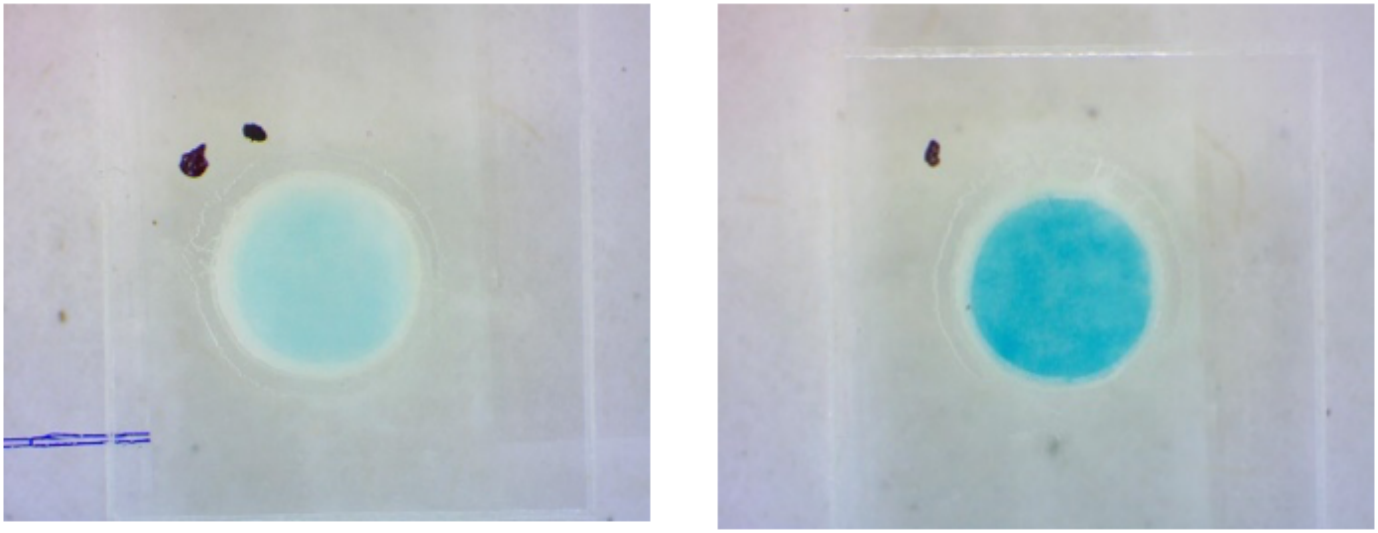

Figure 6

The comparison of images recorded after 20 minutes of incubation with TMB in between in the absence of Rabbit anti-human CD9 (left) and in the presence of Rabbit anti-human CD9 (right)

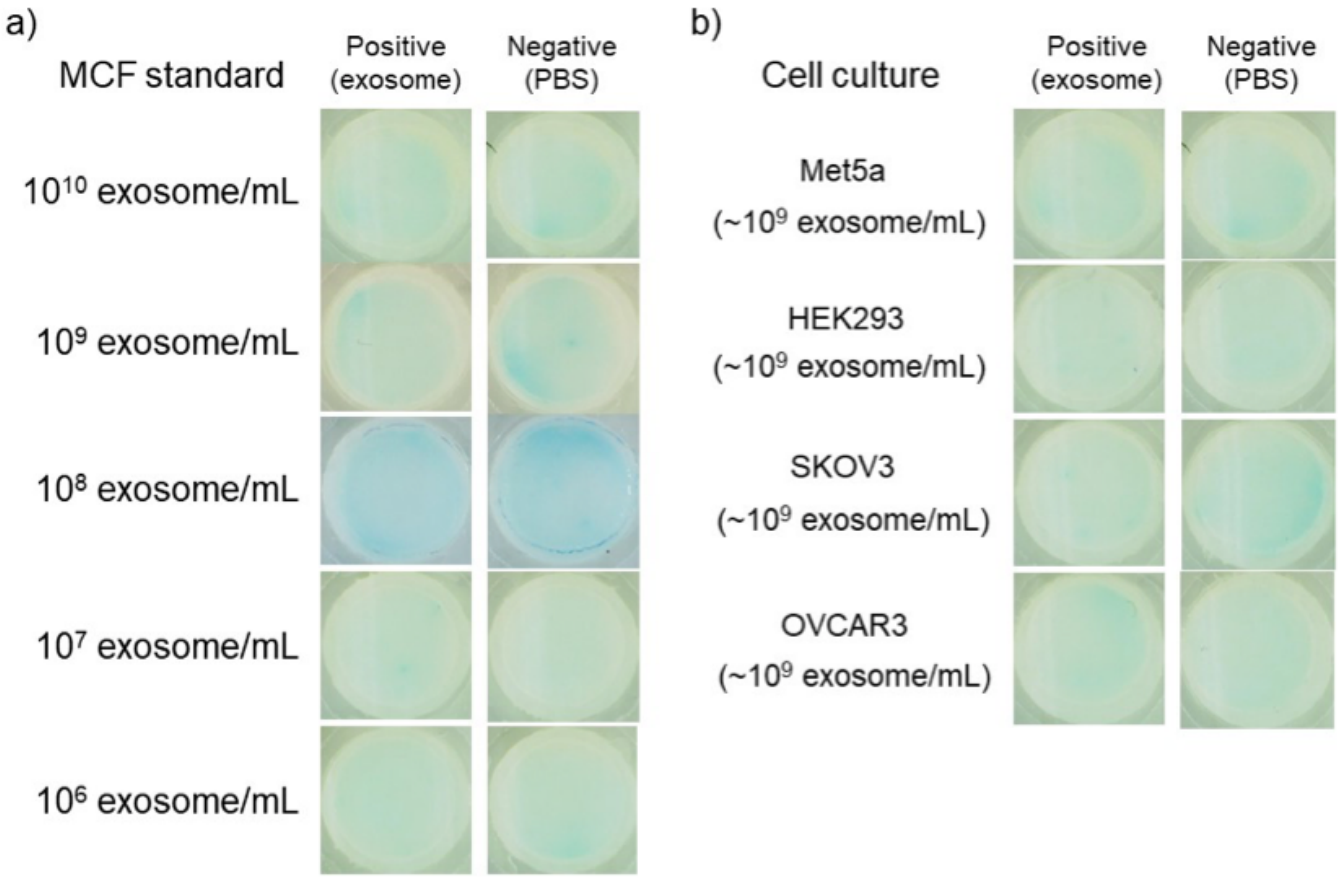

Figure 7

Analytical performance of the assay (a) colorimetric assay images observed at 15th min of MCF standard from a known concentration of 106 to 1010 exosome/mL (b) colorimetric assay images observed at 15th min of exosomes harvested from Met5a, HEK293, SKOV3 and OVCAR3. Both MCF standard and cell culture samples was compared between positive sample containing exosomes and negative control which was PBS. There is no significant difference between negative and positive case.

Supplementary Files

This is a list of supplementary files associated with this preprint. Click to download.

- SupplementaryInformation.docx